RI 9045

Bureau of Mines Report of Investigations/1986

Wood Crib Fires in a Ventilated Tunnel

By Margaret R. Egan and Charles D. Litton

UNITED STATES DEPARTMENT OF THE INTERIOR

Report of Investigations 9045

Wood Crib Fires in a Ventilated Tunnel

By Margaret R. Egan and Charles D. Litton

UNITED STATES DEPARTMENT OF THE INTERIOR
Donald Paul Hodel, Secretary

BUREAU OF MINES
Robert C. Horton, Director

Library of Congress Cataloging in Publication Data:

Egan, Margaret R
Wood crib fires in a ventilated tunnel.

(Report of investigations; 9045)

Bibliography: p. 17.

Supt. of Docs. no.: I 28.23:9045.

1. Mine fires. 2. Mine timbering. 3. Mine ventilation. I. Litton, C. D. (Charles D.). II. Title. III. Series: Report of investigations (United States. Bureau of Mines);9045.

TN23.U43 [TN315] 622 s [622'.8] 86-600181

CONTENTS

ILLUSTRATIONS

TABLES

UNIT OF MEASURE ABBREVIATIONS USED IN THIS REPORT

cfm	cubic foot per minute	m	meter
cm	centimeter	m^2	square meter
g	gram	m^3/s	cubic meter per second
g/cm^3	gram per cubic centimeter	mg/m^3	milligram per cubic meter
g/g	gram per gram	$\mu g/m^3$	microgram per cubic meter
g/m^3	gram per cubic meter	min	minute
$g/(m^3 \cdot ppm)$	gram per (cubic meter times part per million)	μm	micrometer
g/min	gram per minute	p/cm^3	particle per cubic centimeter
g/s	gram per second	pct	percent
kg	kilogram	p/g	particle per gram
kJ/g	kilojoule per gram	ppm	part per million
kW	kilowatt	psi	pound per square inch

WOOD CRIB FIRES IN A VENTILATED TUNNEL

By Margaret R. Egan[1] and Charles D. Litton[2]

ABSTRACT

This Bureau of Mines report presents results from experimental studies on wood crib fires in an intermediate-scale fire tunnel. Gas concentrations, smoke particle characteristics, heat release rates, and ventilation rates were determined. These measurements form a data base for wood, which can be used with previous analyses for coal and future studies of other mine combustibles, to comprehend the potential hazards of these materials in underground mine fires. A knowledge of the combustion products emitted from these materials will benefit fire detection and control.

Results show the changes in burning rate and heat release rate produced by different crib configurations and ventilation rates. Also included are the effects that the burning rate has on smoke characteristics and gas production.

[1]Chemist.
[2]Supervisory physical scientist.
Pittsburgh Research Center, Bureau of Mines, Pittsburgh, PA.

INTRODUCTION

The Bureau of Mines is involved in research to define the characteristics of fires in ventilated mine passageways. This information is important for the detection of such fires and assessing the hazards that these fires produce.

Timber, which is the second most abundant fuel in coal mine fires, is used to support the walls and roofs of mine passageways. In an accident, fire can propagate along these supports, producing such life-threatening hazards as toxic fumes, smoke, and heat. Studies are necessary to determine the properties of burning wood, as well as other mine combustibles, in order to quantify the hazards of fire propagation, combustion product toxicity, and smoke obscuration.

Previous Bureau studies have addressed the hazard of fire propagation within timbered passageways and provided data on the yield of two main combustion products, carbon monoxide (CO) and carbon dioxide (CO_2) (1),[3] and have shown that the intermediate-scale fire tunnel used for the current studies can successfully predict full-scale fire conditions (2).

This report details the results of tests in the intermediate-scale tunnel using wooden cribs ignited by a natural gas burner in the presence of a forced ventilating airflow. Four crib configurations were tested. A major portion of this report addresses the characteristics of smoke particles generated from wood fires. Detection of smoke particles is often used to signal the onset of fire. Furthermore, smoke particles represent a major hazard because of obscuration and their potential contribution to total toxicity. For these reasons, a knowledge of smoke characteristics (mass concentration, number concentration, and average size) is important to assess their potential impact on the detectability of fires and on the toxicity hazard.

This report also gives additional data on CO, CO_2, and burning rates, to be used for comparison with data on other combustible materials.

INSTRUMENTATION

FIRE TUNNEL

The crib fires were conducted in an intermediate-scale fire tunnel located at the Bureau's Pittsburgh Research Center. A diagram of the tunnel is shown in figure 1. The tunnel measures 0.8 m wide by 0.8 m high by 10 m long and is divided into three sections. The first horizontal section begins at the air intake cone, which expands to a hinged portion that can be lifted to allow entrance for the placement of the cribs. Next is the fire zone in which is located the gas burner followed by the crib. The fire zone and the remaining horizontal section are lined with firebrick and instrumented with thermocouples, flow probes, and sampling ports. The diffusing grid begins the vertical portion of the tunnel. Located in this section is an orifice plate that can be manually adjusted to the desired airflow. The final section is horizontal and ends at the exterior exhaust fan.

THERMOCOUPLES

The thermocouple arrays were located 1.57, 2.36, 3.15, 4.72, 6.30, and 7.87 m from the gas burner. Additional thermocouples were located on the intake air side and at the exhaust. In all, a total of 44 thermocouples were used to measure the temperature distributions resulting from the fires.

[3]Underlined numbers in parentheses refer to items in the list of references preceding the appendix.

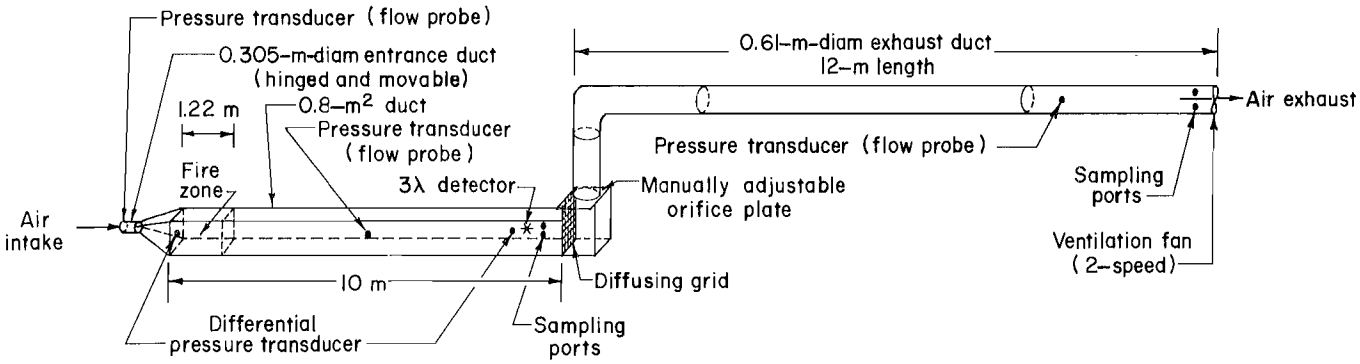

FIGURE 1.—Intermediate-scale fire tunnel.

FLOW PROBES WITH PRESSURE TRANSDUCERS

The air pressure produced by the exhaust ventilation is detected by the transducers. As pressure increases, the capacitance changes. This change is then converted to a linear electric signal. Nonlinearity is described as <±0.1 pct full range of the output or ±0.00001 psi differential. The locations of the pressure transducers are shown in figure 1.

GAS SAMPLING INSTRUMENTATION

The CO analyzer measures accurately within 1 pct of full range, or ±5 ppm. The CO_2 analyzer measures accurately within 1 pct of full range, or ±250 ppm.

PARTICLE SAMPLING INSTRUMENTATION

The number concentration data were obtained with a condensation nuclei monitor, manufactured by Environment One Corp.[4] The monitor measures the concentration of submicrometer airborne particles (p) using a cloud chamber. The particulate cloud attenuates a light beam that ultimately produces a measurable electrical signal. The accuracy is stated as ±20 pct of a point above 30 pct of scale on the linear ranges, 3,000 to 300,000 p/cm^3.

The mass concentration data were obtained by a tapered-element oscillating microbalance, developed by Rupprecht & Patashnick Co., Inc. It measures the mass directly by depositing the particles on a filter attached to an oscillating tapered element. The change in the oscillating frequency of the tapered element is directly proportional to the change in mass. The apparatus is capable of measuring dust concentrations with a better than 10 pct accuracy at the 250-μg/m^3 level.

A three-wavelength light transmission technique was also used to measure smoke concentrations. White light was transmitted through a smoke cloud to the detector. The beam was split into three parts, and each passed through an interference filter centered at wavelengths of 0.45, 0.63, or 1.00 μm. Each photodiode output was amplified and recorded as a linear electric signal. This technique was developed at the Bureau by Cashdollar, Lee, and Singer (3).

WEIGHT LOSS INSTRUMENTATION

The weight loss data were obtained by a strain gauge conditioner in conjunction with a load cell, which has a range up to 22.68 kg. The accuracy of the strain gauge is stated as 0.05 pct of full scale, or ±11.3 g.

[4]Reference to specific equipment does not imply endorsement by the Bureau of Mines.

CRIBS

The cribs were constructed of Douglas fir using a small amount of carpenter's glue for joining. The height and spacing of the sticks were chosen to study the growth and propagation of the fire in four different crib configurations. The configurations and their dimensions are shown in figure 2.

TYPICAL TEST PROCEDURE

The cribs were placed on a stainless steel pan with its shaft extending through the tunnel floor. The shaft was supported on a load cell so that continuous weight loss could be recorded.

Prior to each experiment, background readings were obtained after the crib was positioned, the cone was closed, and the exhaust fan was started. All instruments were simultaneously scanned and recorded by a data logger and a magnetic tape.

A gas jet, located immediately upstream from the pan, was the ignition source. The burner flow rate ranged from 3.5 to 7.0 cfm depending upon the crib configuration and the ventilating airflow (table 1). The burner heat release and ventilation rates are also shown in table 1. Note the decrease in the airflow between induction (ignition of the crib) and the flaming stage. This reduction is caused by the ignition of the crib.

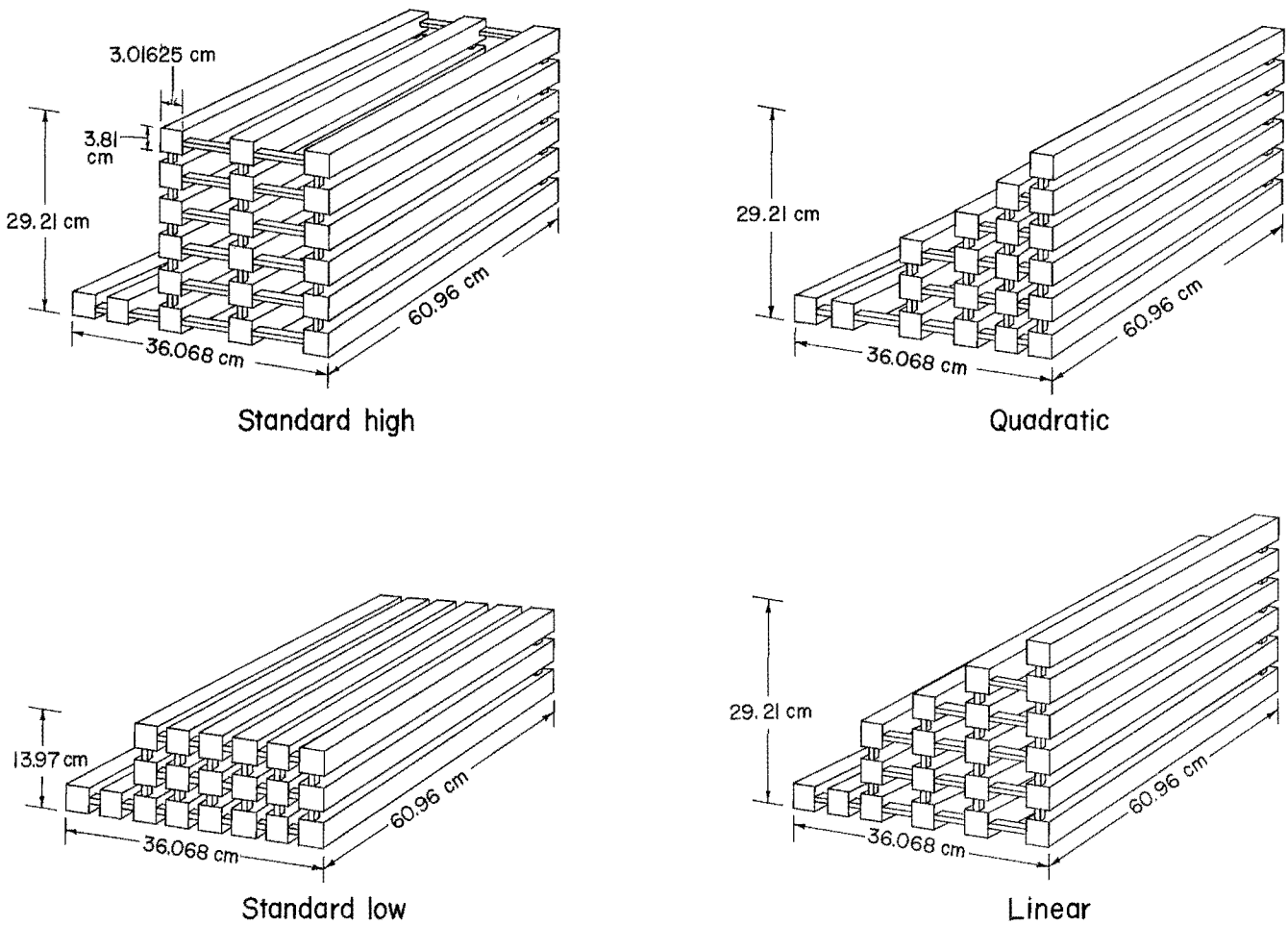

FIGURE 2.—Crib configurations. Air flows from left to right.

TABLE 1. - Experimental conditions

Crib type and test	Burner flow rate, cfm	Burner heat release, kW	Airflow, m^3/s	
			Induction	Flaming
Standard low:				
Test 2.....	5→3.5	82.94	1.0884	1.0525
Test 4.....	5→6	95.77	1.0742	1.0363
Quadratic:				
Test 1.....	6→7	106.87	1.0747	1.0279
Test 8.....	6→5	93.32	.8548	.8211
Standard high:				
Test 3.....	5→4.5	83.36	1.0864	1.0471
Test 7.....	6→4.5	97.49	.4898	.4859
Linear:				
Test 5.....	5→6→5.5→7	97.36	1.0600	1.0018
Test 6.....	6→5	100.75	.6534	.6167

→ Flow rate change.

Once the crib ignited, the burner was turned off. The fire propagated, consuming all the available wood fuel. When the CO concentration returned to the background level, the experiment was concluded.

THEORY

It has been shown (4) that the total heat release rate realized during a fire can be calculated from the expression

$$\dot{Q}_A = \left(\frac{H_C}{K_{CO_2}}\right)\dot{G}_{CO_2} + \left(\frac{H_C - H_{CO}\,K_{CO}}{K_{CO}}\right)\dot{G}_{CO}, \qquad (1)$$

where H_C = net heat of complete combustion of the fuel, kJ/g;

H_{CO} = heat of combustion of CO = 10.1 kJ/g;

K_{CO_2} = stoichiometric yield of CO_2, g/g;

K_{CO} = stoichiometric yield of CO, g/g;

$\dot{G}_{CO_2}$ = generated rate of CO_2, g/s;

$\dot{G}_{CO}$ = generated rate of CO, g/s;

and $\dot{Q}_A$ = actual heat release rate, kW.

In a ventilated system, the generation rates ($\dot{G}$) of CO_2 and CO are related to the bulk average concentration (M) increases above ambient, ΔCO_2 and ΔCO, by the expressions

$$\dot{G}_{CO_2} = M_{CO_2}\, V_o A_o\, \Delta CO_2 \qquad (2)$$

and

$$\dot{G}_{CO} = M_{CO}\, V_o A_o\, \Delta CO, \qquad (3)$$

where $M_{CO_2} = 1.97 \times 10^{-3}$ g/(m^3·ppm);

$M_{CO} = 1.25 \times 10^{-3}$ g/(m^3·ppm);

and $V_o A_o$ = incoming cold gas flow, m^3/s.

For Douglas fir used in these experiments, H_C equals 16.4 kJ/g, K_{CO_2} equals 1.723 g/g, and K_{CO} equals 1.097 g/g. Substituting these values and equations 2 and 3 into equation 1 yields

$$\dot{Q}_A = V_o A_o\,[0.01875\,(\Delta CO_2) + 6.06 \times 10^{-3}\,(\Delta CO)]. \qquad (4)$$

Continuous measurements of $V_o A_o$, ΔCO_2, and ΔCO during these experiments allowed

for the calculation of the actual heat release rates of each experiment using equation 4.

A typical fire rarely realizes the state of complete combustion, and for this reason, the actual heat of combustion during a fire is usually less than the total heat of combustion, H_C. By measuring both the actual heat release rate, equation 4 above, and the fuel mass loss rate ($\dot{M}_f$) using the load cell assembly, the actual heat of combustion can be calculated from

$$H_A = \dot{Q}_A/\dot{M}_f, \tag{5}$$

which, in turn, allows calculation of the fraction of the total heat of combustion realized in a fire:

$$F_A = H_A/H_C. \tag{6}$$

COMBUSTION PRODUCT YIELDS

The yield of a combustion product, X, is related to the mass burning rate (assumed equal to the fuel mass loss rate) and to the measured bulk average concentration increases above ambient, ΔX, by the expression

$$C_X(\Delta X) = Y_X(\dot{M}_f)/V_oA_o, \tag{7}$$

where

Y_X = true yield of the combustion product, g/g [for gases and mass concentration of smoke particles (M_o)] or p/g [for number concentration of smoke particles (N_o)];

ΔX = standard concentration increase, ppm (for product gas), mg/m^3 [for smoke particles (M_o)], or p/cm^3 [for smoke particles (N_o)];

and

C_X = appropriate units conversion factor:
1.97×10^{-3} when CO_2 is in ppm,
1.25×10^{-3} when CO is in ppm,
1.00×10^{-3} when M_o is in mg/m^3,
or
1.00×10^{6} when N_o is in p/cm^3.

When $\dot{M}_f$, ΔX, and V_oA_o are measured, the true yield can be calculated from equation 7 directly. However in situations where $\dot{M}_f$ is not measured but Q_A is known, a maximum yield can be calculated by assuming $\dot{M}_f = \dot{Q}_A/H_C$, i.e., complete combustion.

In a typical mine fire, it is often difficult, if not impossible, to know the actual heat of combustion. Moreover, since the true yield of a combustion product depends upon this information, significant errors can result in predicting the resultant concentration increases. For flaming fires, the relative hazards tend to increase with the actual heat release rate that results.

For this reason, it is convenient to define a parameter, β_X, for a given product by

$$\beta_X = \frac{(Y_X)_{max}}{H_C}. \tag{8}$$

The resultant concentration increase may be expressed by either of the following two relationships, one for complete combustion:

$$C_X(\Delta X) = \frac{(Y_X)_{max}\ \dot{Q}_A/H_C}{V_oA_o}, \tag{9}$$

and one for actual combustion by combining equations 5 and 7:

$$C_X(\Delta X) = \frac{Y_X\ \dot{Q}_A/H_A}{V_oA_o}; \tag{10}$$

therefore, it is clear that

$$\beta_X = \frac{(Y_X)_{max}}{H_c} = \frac{Y_X}{H_A}, \tag{11}$$

where β_X is independent of the true yield or actual heat of combustion, but the resultant product levels, $C_X(\Delta X)$, reflect only fire size, $\dot{Q}_A$.

SMOKE PARTICLES

Measurements of both smoke number concentrations and smoke mass concentrations provide important information relative to the yields (or β-values) of these quantities during actual fires. These measurements can also provide information relative to the average size of the particles.

If N_o is the number concentration of smoke particles (in particles per cubic centimeter) and M_o is the mass concentration of smoke particles (in milligrams per cubic meter) measured at any time, t, then the following relationship holds:

$$\left(\frac{\pi d_m^3}{6}\right) \rho_p N_o = 1 \times 10^3 M_o, \quad (12)$$

where ρ_p = individual particle density, g/cm^3;

d_m = mass mean diameter of the particle, μm;

and 1×10^3 = the appropriate units conversion factor.

Assuming a value of $\rho_p = 1.4$ g/cm^3, then the diameter of the particles can be calculated from

$$d_m = 11.09 \left(\frac{M_o}{N_o}\right)^{1/3}, \quad (13)$$

where the particle diameter is expressed in micrometers.

GENERAL RESULTS

The burning rate of each crib was divided into three stages determined by mass loss. In the ignition stage, the natural gas burner igniting the crib accounts for the slight mass loss. After the crib ignited, the burner was turned off. In the flaming stage, the burning crib is consuming most of the available fuel, which produces the greatest mass loss, heat, and CO_2. Following intense burning is the decaying stage when most of the CO is produced. At this time, the crib had generally been burned to 84 pct completion and only a low-level postflame smoldering remained. Table 2 shows the time of ignition, the length of the

TABLE 2. - Experimental data for ignition time, steady-state burning time, and mass loss rate

Crib type and test	Ignition time, min	Steady-state burning time, min	Mass loss rate, g/min		
			Ignition	Flaming	Decaying
Standard low:					
Test 2.....	8.1	15.3	28.9	448.86	13.96
Test 4.....	14.68	15.62	17.65	412.96	26.65
Quadratic:					
Test 1.....	6.42	10.08	19.9	647.5	17.3
Test 8.....	9.23	15.7	15.41	529.87	5.75
Standard high:					
Test 3.....	3.6	10.8	38.31	725.35	5.7
Test 7.....	4.6	12.0	63.51	668.14	16.72
Linear:					
Test 5.....	9.75	8.92	35.38	778.62	5.59
Test 6.....	6.0	6.7	48.99	769.68	13.43

maximum mass loss or flaming stage, and the mass loss slopes for each experiment.

Graphs depicting heat release, mass loss, CO, CO_2, mass and number concentrations, and mass mean diameter for the eight tests are shown, as a function of time from the ignition of the gas burner, in figures 3-10.

GAS CONCENTRATIONS

CO, a product of incomplete combustion, reaches its highest level in the decaying stage. Approximately 21 min after the crib ignited, the average maximum concentration of 378 ppm was achieved. Generated CO levels, at this time, averaged

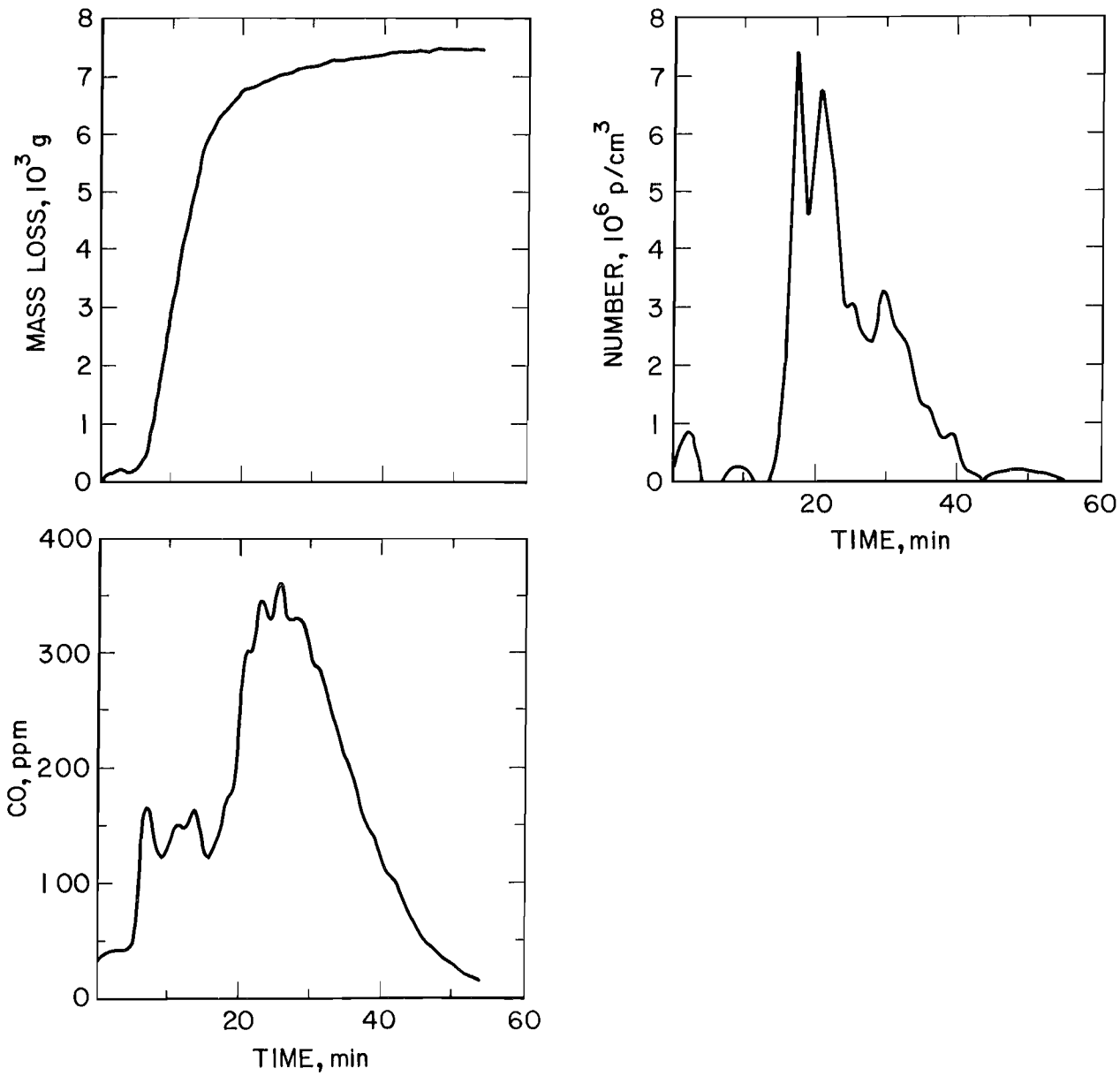

FIGURE 3.—Test 1, quadratic crib. (Heat release, CO_2, mass, and mean diameter were not determined.)

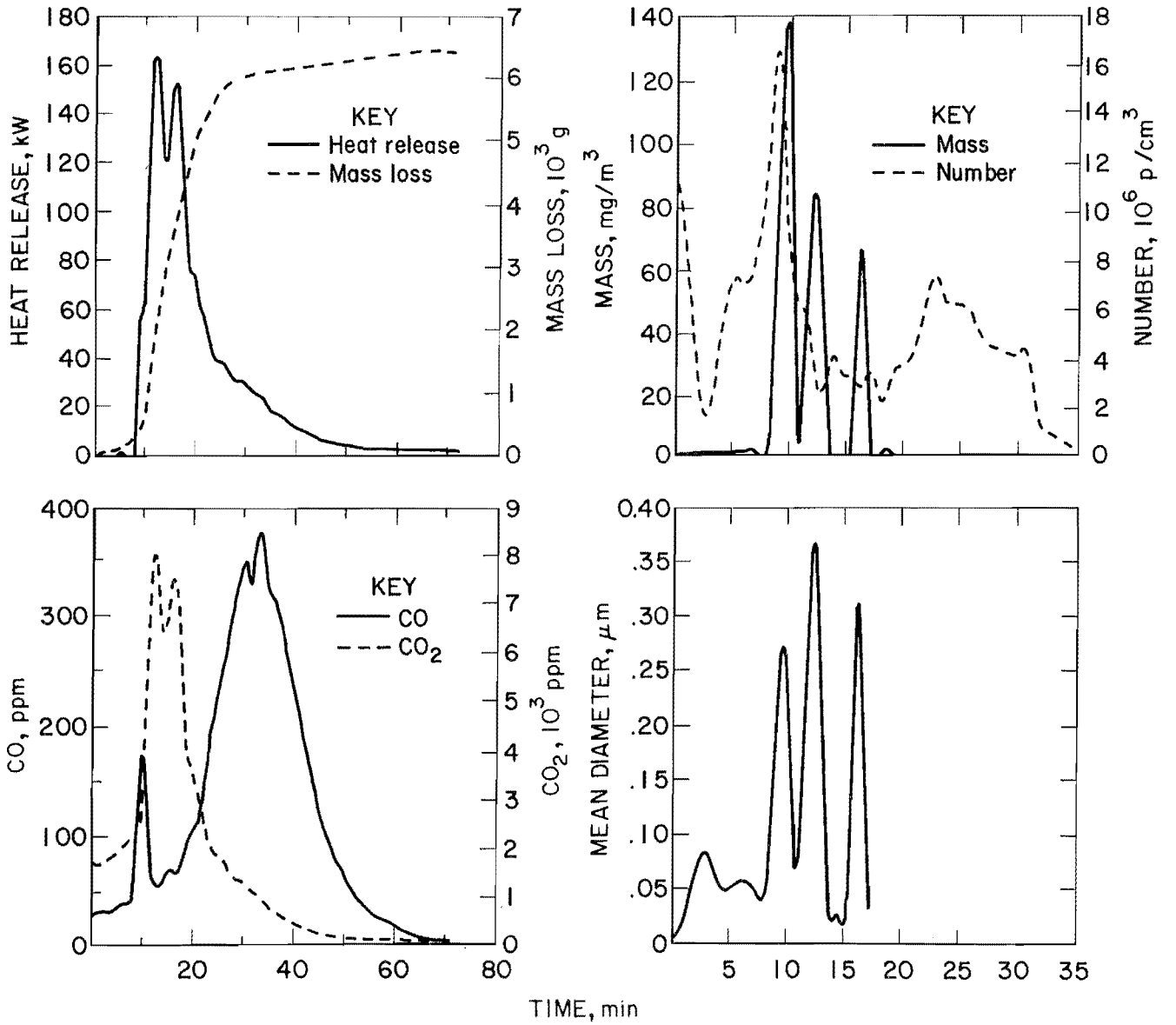

FIGURE 4.—Test 2, standard low crib.

0.3883 g/s, corresponding to an average yield of 0.56932 g/g. For all eight experiments, the concentration of CO throughout the flaming stage averaged 145 ppm, corresponding to an average yield of 0.0158 g/g. The yield of CO in the decaying stage was a 37-fold increase over this.

The highest concentrations of CO_2 were produced during the flaming stage subsequent to ignition, when the fuel is consumed at its maximum rate. The average yield of CO_2 for all the tests during this stage was 1.1217 g/g, which is 65 pct of the stoichiometric value. During the decaying stage, there is only smoldering without flame, but the yields of CO_2 averaged about 2.1 g/g. The average ratios of CO_2 to CO concentration can be calculated from their yields by the expression

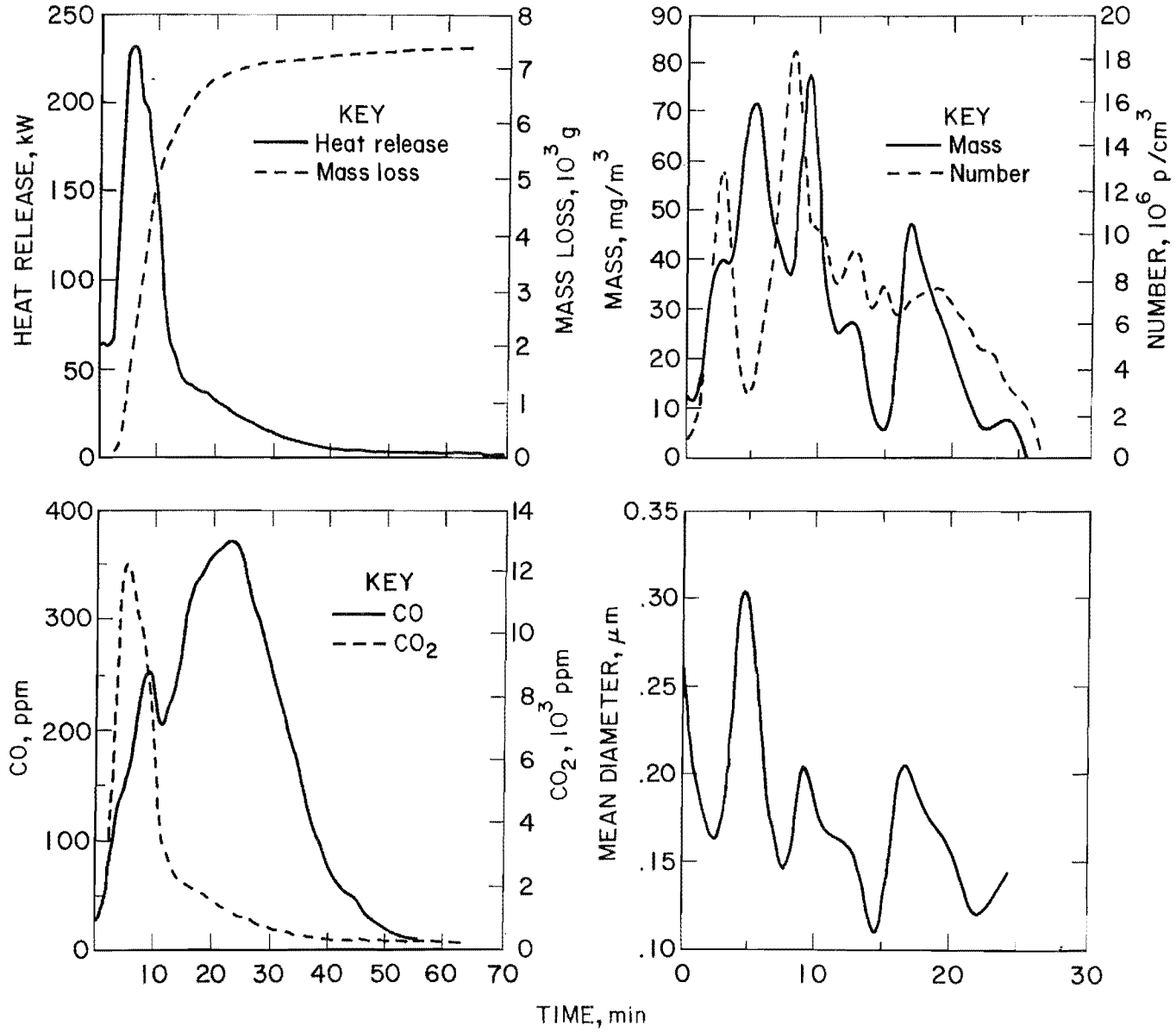

FIGURE 5.—Test 3, standard high crib.

$$\frac{CO_2}{CO} = \frac{1.25 \times 10^{-3}}{1.97 \times 10^{-3}} \frac{Y_{CO_2}}{Y_{CO}} = 0.635 \frac{Y_{CO_2}}{Y_{CO}}. \qquad (14)$$

During the rapid combustion stage, this ratio has an average value of 45, and it decreases during the decaying stage to 3.5. Clearly, during the latter portion of the decaying stage, this ratio is even lower because of the cooler temperatures of the smoldering wood, which are insufficient to convert CO to CO_2. Values of 1 to 2 for this ratio would be indicative of this advanced decaying stage.

This ratio can be used to determine the approximate stage of combustion: low values of the ratio reflect smoldering combustion stages while high values reflect intense, flaming combustion. Further, the absolute levels of CO and CO_2 measured during a flaming fire may be used to calculate the fire size provided the ventilation in the affected entry is known. Both of these parameters (size

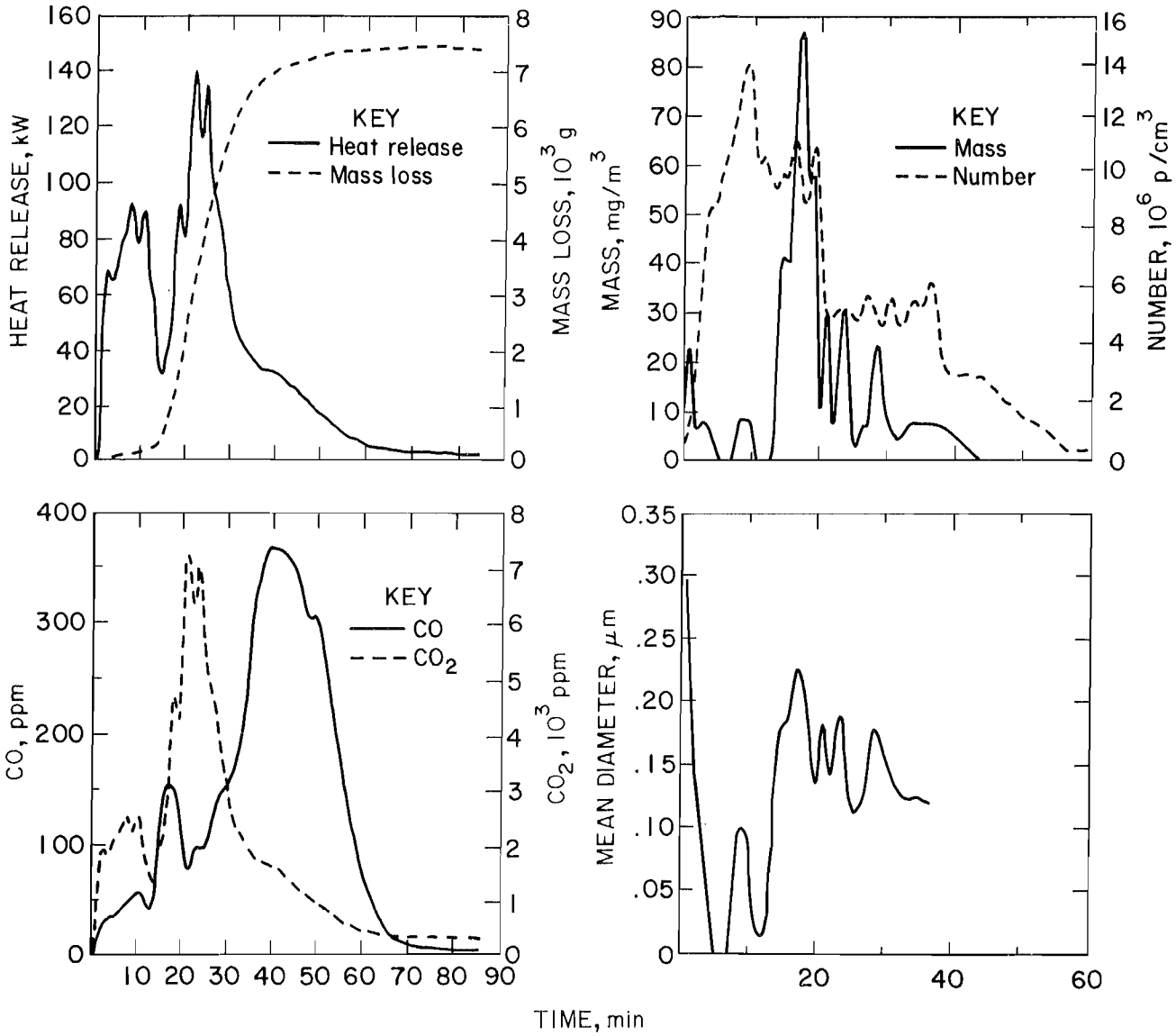

FIGURE 6.—Test 4, standard low crib.

and combustion stage) are often of significant importance during mine fire emergencies.

SMOKE CHARACTERISTICS

Each stage of combustion produces slightly different smoke particle characteristics. The ignition and decaying stages yielded approximately 6×10^{12} p/g of smoke with a mass mean diameter of 0.17 μm. The mass yield in the ignition stage was 0.0205 g/g, about the same as the decaying stage yield of 0.0236 g/g. In the flaming stage, a cleaner burning fire produced 5×10^{11} p/g of smoke with a mass yield of 0.0042 g/g. Relatively low yields are expected because of the rapid burning rate during this stage.

The most smoke particles were produced approximately 10 min after ignition, when the average maximum number of particles was 1.53×10^7 p/cm^3. This corresponds to an average yield of 2.36×10^{12} p/g. The average number during the flaming stage was 6.04×10^6 p/cm^3, which corresponds to an average yield of 5.16×10^{11} p/g. Table 3 shows the actual number concentrations.

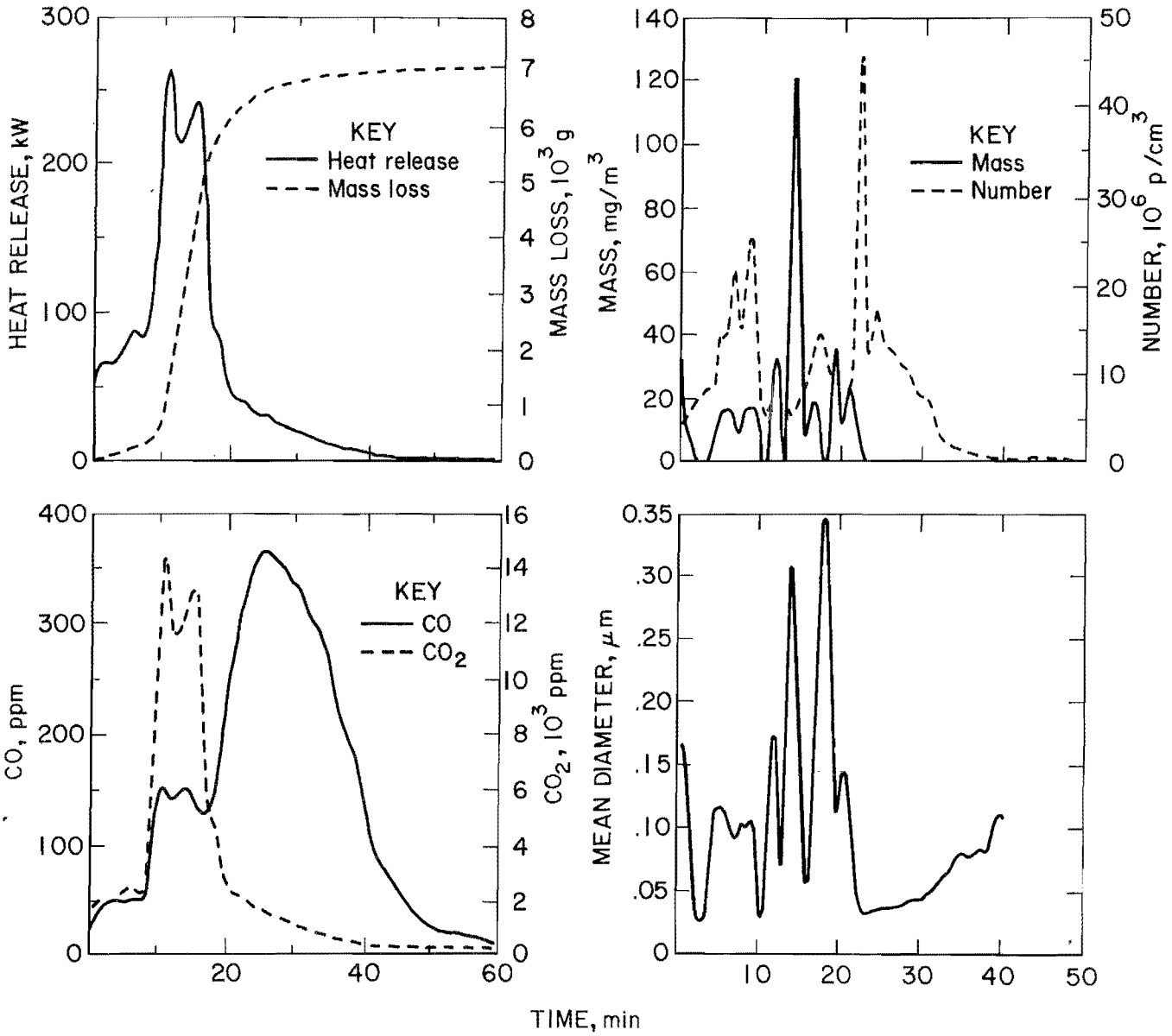

FIGURE 7.—Test 5, linear crib.

TABLE 3. - Number concentrations, particles per cubic centimeter

Crib type and test	Ignition stage			Flaming stage			Decaying stage		
	High	Average	Low	High	Average	Low	High	Average	Low
Standard low:									
Test 2.....	1.18×10^7	7.37×10^6	1.45×10^6	1.73×10^7	5.26×10^6	1.85×10^6	6.15×10^6	3.46×10^6	3.50×10^5
Test 4.....	1.43×10^7	9.58×10^6	1.19×10^6	1.24×10^7	7.20×10^6	4.59×10^6	6.39×10^6	2.36×10^6	3.80×10^4
Quadratic:									
Test 1.....	6.75×10^5	2.97×10^5	5.50×10^4	4.33×10^6	1.13×10^6	3.00×10^4	7.83×10^6	2.56×10^6	2.40×10^3
Test 8.....	1.29×10^7	5.97×10^6	2.81×10^6	1.80×10^7	8.09×10^6	4.98×10^6	6.68×10^6	2.69×10^6	1.90×10^4
Standard high:									
Test 3.....	1.34×10^7	6.24×10^6	9.90×10^5	1.86×10^7	9.06×10^6	2.78×10^6	7.59×10^6	5.05×10^6	3.30×10^5
Test 7.....	5.26×10^6	3.67×10^6	2.55×10^6	3.99×10^6	3.24×10^6	2.49×10^6	5.19×10^6	2.47×10^6	1.20×10^5
Linear:									
Test 5.....	2.55×10^7	1.28×10^7	5.08×10^6	1.67×10^7	9.02×10^6	4.72×10^6	4.89×10^7	8.23×10^6	1.43×10^5
Test 6.....	1.05×10^7	6.96×10^6	2.52×10^6	1.40×10^7	5.31×10^6	4.26×10^6	8.51×10^6	4.09×10^6	1.95×10^5

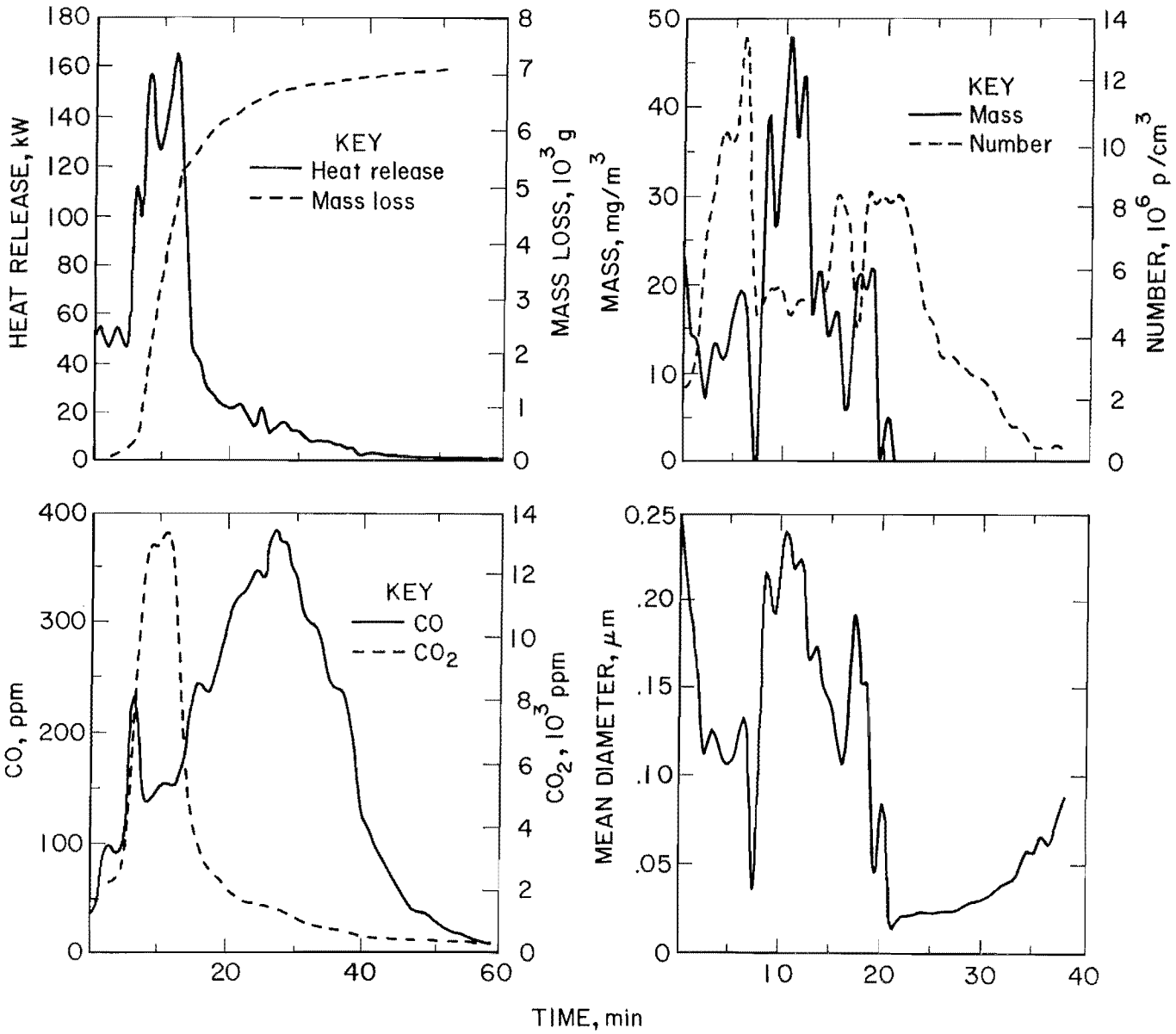

FIGURE 8.—Test 6, linear crib.

The largest mass of particles was produced approximately 4 min after ignition of the crib. At that time the average maximum mass was 104 mg/m^3, corresponding to an average yield of 0.011 g of particles per gram of wood consumed. The average mass throughout the flaming stage was 49.12 mg/m^3, corresponding to an average yield of 0.0042 g/g. Actual mass concentration values can be found in table 4.

The mass mean diameter during the flaming stage averaged 0.223 μm. Mass mean diameter values for each experiment can be found in table 5. In some experiments, the mass concentration and the mass mean diameter in the decaying stage did not exceed background levels, although high concentrations were measured. This would indicate very small particles, for which the mass concentration would be low.

HEAT RELEASE RATES

The initial increase on each heat release curve is due to the gas burner, which was turned off at ignition. The fire size of the gas burner ($\dot{Q}_B$) for each experiment can be found in table 1 and is

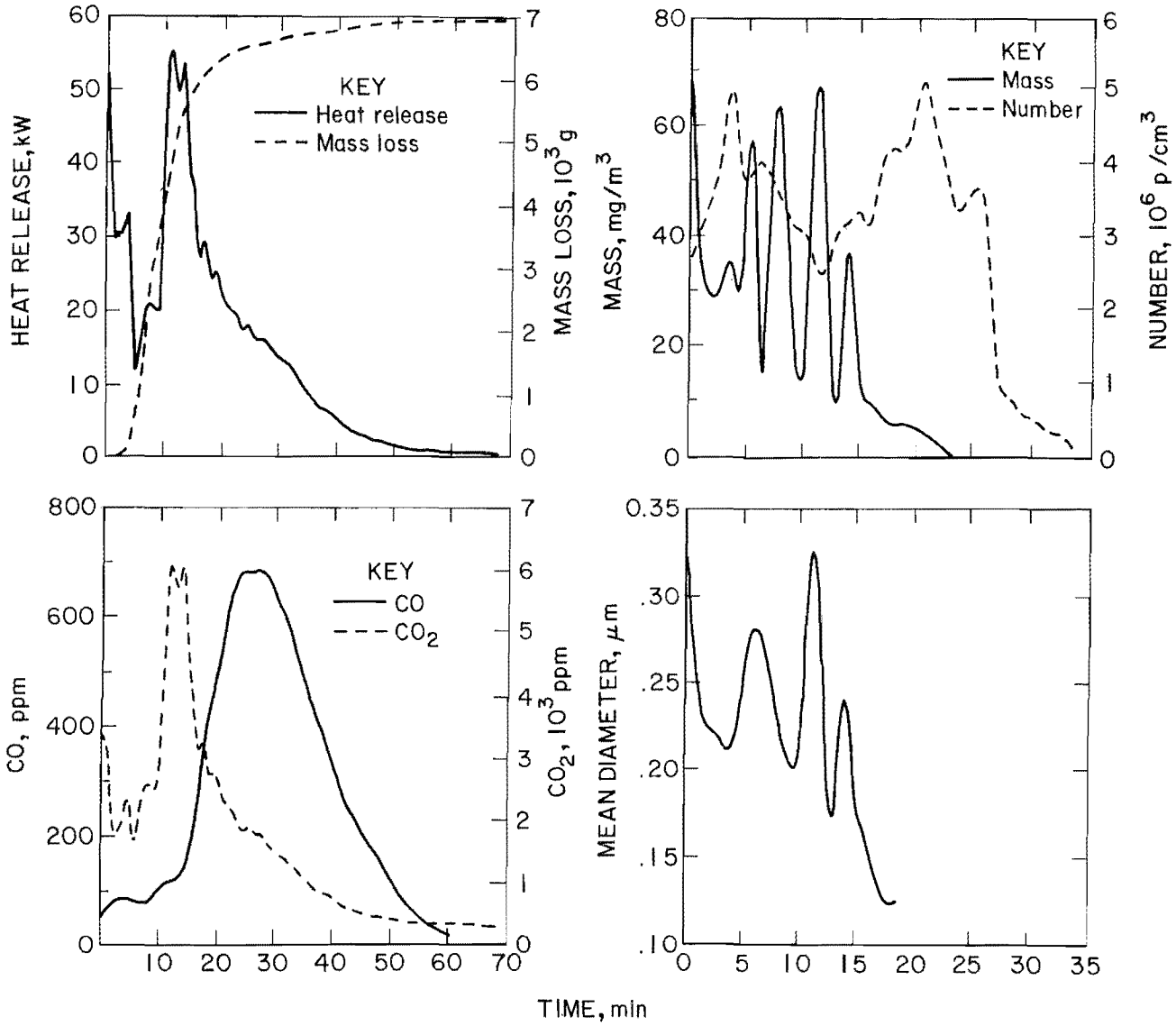

FIGURE 9.—Test 7, standard high crib.

TABLE 4. - Mass concentrations, milligrams per cubic meter

Crib type and test	Ignition stage			Flaming stage			Decaying stage		
	High	Average	Low	High	Average	Low	High	Average	Low
Standard low:									
Test 2.....	0	0	0	137.69	82.84	68.95	0	0	0
Test 4.....	23.98	10.35	8.02	88.25	31.40	7.88	7.85	7.83	7.81
Quadratic:									
Test 1.....	ND	ND	ND	ND	ND	ND	ND	ND	ND
Test 8.....	105.12	35.91	8.79	180.01	84.99	7.84	0	0	0
Standard high:									
Test 3.....	40.48	25.26	13.39	68.31	40.90	6.04	46.89	21.12	6.06
Test 7.....	74.28	41.86	29.67	68.54	33.38	8.62	5.9	5.9	5.9
Linear:									
Test 5.....	47.43	16.85	8.13	124.58	38.62	8.23	39.72	19.34	8.29
Test 6.....	27.80	14.51	6.40	48.49	31.70	10.34	22.25	15.15	5.57

ND Not determined.

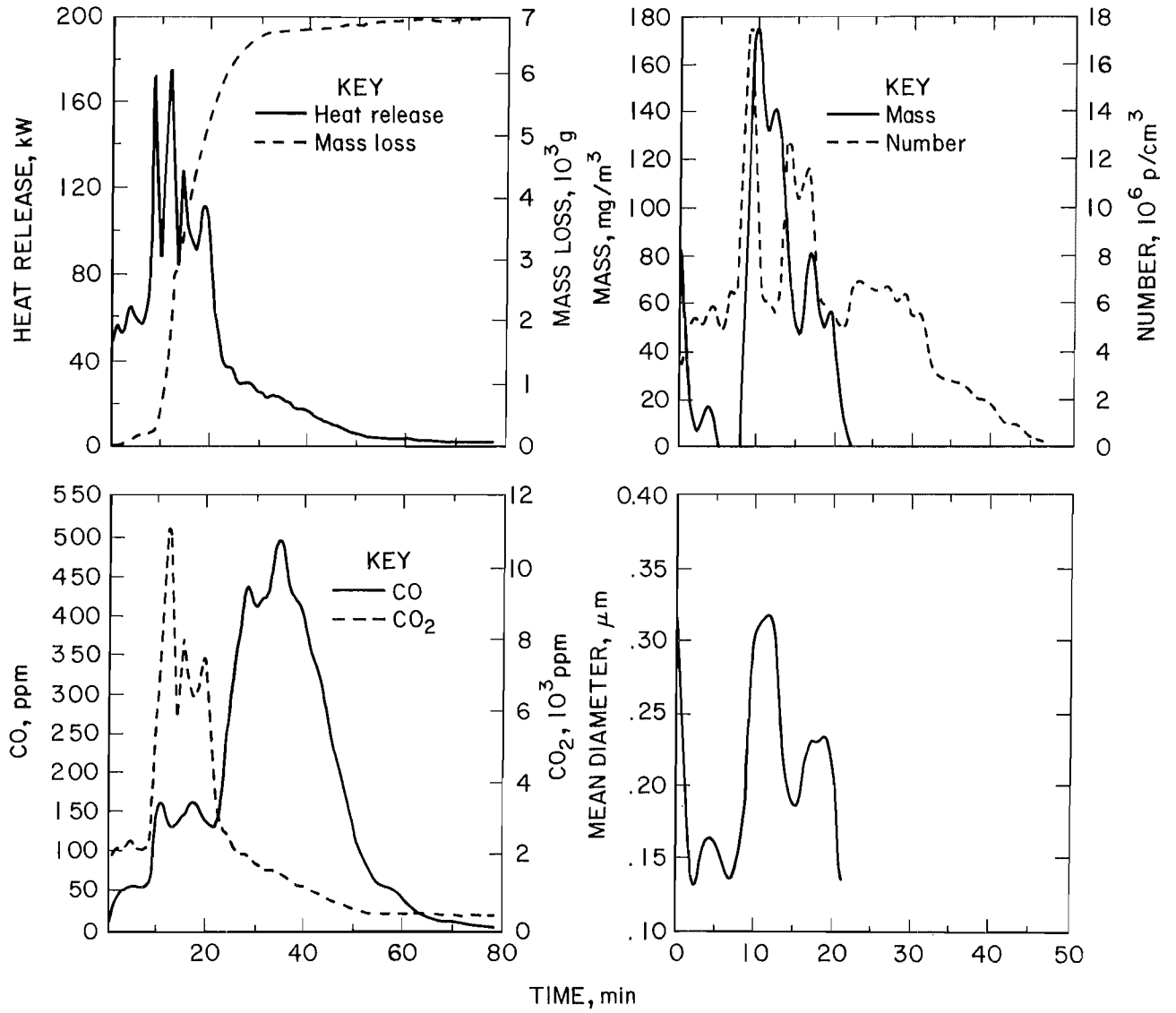

FIGURE 10.—Test 8, quadratic crib.

TABLE 5. - Mass mean diameters, micrometers

Crib type and test	Ignition stage			Flaming stgae			Decaying stage		
	High	Average	Low	High	Average	Low	High	Average	Low
Standard low:									
Tets 2.....	0	0	0	0.361	0.278	0.176	0	0	0
Test 4.....	.302	.114	.092	.232	.181	.110	.126	.121	.119
Quadratic:									
Test 1.....	ND	ND	ND	ND	ND	ND	ND	ND	ND
Test 8.....	.371	.202	.131	.318	.243	.129	0	0	0
Standard high:									
Test 3.....	.264	.177	.160	.322	.183	.101	.210	.179	.144
Test 7.....	.341	.250	.210	.335	.241	.155	.125	.125	.124
Linear:									
Test 5.....	.163	.122	.090	.330	.180	.113	.174	.147	.062
Test 6.....	.246	.142	.107	.245	.201	.123	.204	.172	.098

ND Not determined.

TABLE 6. - Heat release rates during the flaming stage

Crib type and test	Heat release rate ($\dot{Q}_A$), kW	Heat of combustion (H_A), kJ/g	Crib type and test	Heat release rate ($\dot{Q}_A$), kW	Heat of combustion (H_A), kJ/g
Standard low:			Standard high:		
Tets 2.....	98.16	13.12	Test 3.....	142.81	11.81
Test 4.....	84.62	12.30	Test 7.....	31.73	2.85
Quadratic:			Linear:		
Test 1.....	ND	ND	Test 5.....	191.32	14.74
Test 8.....	91.86	10.40	Test 6.....	131.07	10.22

ND Not determined.

calculated from equation 4 of the previous section.

During the flaming stage, large amounts of heat are generated from the combustion of the volatile gases emerging from the burning fuel. Table 6 shows these values during the flaming or maximum mass loss stage.

DISCUSSION OF RESULTS

CRIB CONFIGURATION

The configuration of the crib significantly affected the maximum mass loss time and the mass loss slope in the flaming stage, as shown in table 2. The spacing of the sticks in the linear crib permitted the most efficient heat transfer, which produced the most rapid mass loss. Lowering the profile of the crib decreased the mass loss rate and lengthened the time of ignition. The high crib ignited and burned faster than the low crib. Decreasing the angle at which the sticks are positioned increased the mass loss rate but did not effect the time of ignition. The quadratic and linear cribs ignited at about the same time, but the linear crib, with a lower angle and a more efficient heat transfer, burned faster.

VENTILATION FLOW RATE

The flow rates for experiments 1 through 5 were held constant at 1,770 cfm (approximately 1 m^3/s). In experiments 6, 7, and 8, lower ventilation rates were used. A corresponding decrease in the average yield of CO_2 and CO (Y_{CO_2} and Y_{CO}), during the flaming stage, was observed as follows:

Tests	Airflow rate, m^3/s	Y_{CO_2}, g/g	Y_{CO}, g/g
1-5..	~1.0	1.3502	0.0183
8....	.82	1.0847	.0188
6....	.62	1.0703	.0098
7....	.49	.2961	.0065

Decreasing the ventilation flow decreases the rate at which oxygen is supplied to the fire. At reduced oxygen, the flame burns in a more fuel-rich state, as evidenced by the reduced yields of CO_2.

Low yields of CO in tests 6 and 7 may be a result of stratification of the gases in the tunnel caused by the lowered airflow. For these tests, the bulk of the CO may have remained near the roof. The concentrations obtained at the midpoint sampling port may be significantly lower than the true concentration. For test 7, the low yield of CO_2 may also be a result of insufficient mixing.

Decreasing the ventilation decreased the mass and number yield of particulates, but increased their mass mean diameter. At the lower ventilation rates, fewer and lighter smoke particles are produced, but the particles have a larger mass mean diameter. Two possible explanations for this phenomenon are (1) a slower transport time coagulates the

particles or (2) incomplete combustion produces larger particles.

Burning the same crib configuration at an increased ventilation rate or air velocity resulted in a faster burning rate. In the range tested, higher air velocities increased the burning rate by making more oxygen available for combustion and by increasing the efficiency of the heat transfer. The same effect was observed in a Factory Mutual report (4). Their burning rates reached a maximum at flows between 2 and 3 m^3/s. Beyond this point, convective cooling competes with the heat transfer and slows the burning rate.

SMOKE CHARACTERISTICS

The burning rate affects the smoke particle characteristics. Slower burning cribs produce more smoke (larger particle mass and number) than do faster burning ones, but the particle size (mass mean diameter) remains the same. This may be a consequence of incomplete combustion.

The mechanism for the information of smoke particles differs for each combustion stage. The largest number yield of particles is found in the ignition and decaying stages. But particles with the largest mass mean diameter are produced in the flaming stage. Rapid oxidation yields a cleaner burning fire with less smoke and toxic gas production.

When the smoke characteristics from wood fires are compared with smoke characteristics from previous coal fire studies (5), the data indicate that three times the fire size of wood is required to produce the same mass, number, and obscuration rate as that obtained for coal. Coal generates a denser, more hazardous, but more detectable fire than wood. In areas heavily loaded with wood, only very sensitive smoke detectors would be effective. In addition to producing denser smoke, coal fires generate more toxic gas than do comparably sized wood fires. During the flaming stage, coal fires yield 3 to 5 times more CO than do wood fires.

CONCLUSIONS

These experiments measured the gas concentrations and smoke characteristics of wood crib fires in a ventilated tunnel. Also investigated was the effect that crib configuration and ventilation rate have on combustion products and burning rates. The resulting data, used with previous coal analyses and future studies of other mine combustibles such as brattice cloth and conveyor belting, can determine possible hazards in underground mine fires. The study of heat, smoke, and toxic gas generated from burning these commonly found substances is basic to developing instrumentation to detect such fires. The ultimate purpose of such research is to prevent loss of life and minimize property damage through early fire detection.

REFERENCES

1. Tewarson, A., and J. S. Newman. An Experimental Investigation of the Fire Hazards Associated With Timber Sets in Mines. Paper in Underground Metal and Nonmetal Fire Protection. Proceedings: Bureau of Mines Technology Transfer Seminars, Denver, Colo., Nov. 3, 1981, and St. Louis, Mo., Nov. 6, 1981. BuMines IC 8865, 1981, pp. 86-103.

2. Lee, C. K., R. F. Chaiken, J. M. Singer, and M. E. Harris. Behavior of Wood Fires in Model Tunnels Under Forced Ventilation Flow. BuMines RI 8450, 1980, 58 pp.

3. Cashdollar, K. L., C. K. Lee, and J. M. Singer. Three-Wavelength Light Transmission Technique To Measure Smoke Particle Size and Concentration. Appl. Opt., v. 18, No. 11, 1979, pp. 1763-1769.

4. Tewarson, A. Analysis of Full-Scale Timber Fire Sets in a Simulated Mine Gallery. Factory Mutual Res. Corp., Norwood, MA, Tech. Reps. J. I. OEON1.RA and J. I. OFON3.RA, June 1982, 55 pp.

5. Litton, C. D., M. Hertzberg, and A. L. Furno. Fire Detection Systems in Conveyor Belt Haulageways. BuMines RI 8632, 1982, 26 pp.

APPENDIX.--LIST OF SYMBOLS

C_X	conversion factor of a combustion product
d_m	mass mean diameter, μm
F_A	fraction of the total heat of combustion
$\dot{G}_{CO}$	generated rate of CO, g/s
$\dot{G}_{CO_2}$	generated rate of CO_2, g/s
H_A	actual heat of combustion, kJ/g
H_C	net heat of combustion of the fuel, kJ/g
H_{CO}	heat of combustion of CO, kJ/g
K_{CO}	stoichiometric yield of CO, g/g
K_{CO_2}	stoichiometric yield of CO_2, g/g
M_{CO}	density of CO, g/(m^3·ppm)
M_{CO_2}	density of CO_2, g/(m^3·ppm)
$\dot{M}_f$	mass loss rate of the fuel, g/s
M_o	mass concentration of smoke particles, mg/m^3
N_o	number concentration of smoke particles,
$\dot{Q}_A$	actual heat release rate, kW
$\dot{Q}_B$	actual heat release rate of the burner, kW
V_oA_o	ventilation rate, m^3/s
Y_{CO}	yield of CO, g/g
Y_{CO_2}	yield of CO_2, g/g
Y_X	yield of a combustion product, g/g or p/g
ΔX	measured change in a given quantity
λ	wavelength, μm
β_X	grams of product per unit kilojoule of heat release
ρ_p	individual particle density, g/m^3

☆ U.S. GOVERNMENT PRINTING OFFICE: 1986—605-017/40,077

INT.-BU.OF MINES,PGH.,PA. 28346